Journal of Aerosol Science 42 (2011) 462–473

Contents lists available at ScienceDirect

Journal of Aerosol Science

journal homepage: www.elsevier.com/locate/jaerosci

A cost-effective differential mobility analyzer (cDMA) for multiple DMA column applications

Fan Mei [a], Huijing Fu [b], Da-Ren Chen [b,*]

[a] Atmospheric Science Division, Brookhaven National Laboratory, 75 Rutherford Drive, Upton, NY 11973-5000, USA
[b] Department of Energy, Environmental and Chemical Engineering, Washington University in St. Louis, Campus Box 1180, One Brookings Drive, St. Louis, MO 63130, USA

ARTICLE INFO

Article history:
Received 28 January 2011
Received in revised form
13 April 2011
Accepted 15 April 2011
Available online 4 May 2011

Keywords:
Cost-effective differential mobility analyzer
Macromolecules
Transfer function
Size resolution
Transmission efficiency

ABSTRACT

In aerosol research and applications, a differential mobility analyzer (DMA) is now considered the standard tool for sizing and classifying monodisperse particles in the sub-micrometer and nanometer size ranges. However, DMA application at the pilot or industrial production scale remains infeasible because of the low mass throughput. A simple way to scale up DMA operation is to use multiple DMA columns. The manufacture and maintenance costs of existing DMAs, however, limit such a scale-up. A cost-effective DMA column (named cDMA) has thus been developed in this work to address the above issue. To reduce its manufacturing cost, the prototype was constructed using parts requiring little machining. The cDMA column was also designed for easy maintenance and easy variation of the classification length for any application-specified size range. In this study, prototypes with two particle classification lengths, 1.75 and 4.50 cm, were constructed and their performance was experimentally evaluated at sheath-to-aerosol flowrate ratios of 5:1, 10:1, and 15:1 via the tandem DMA (TDMA) technique. It was concluded that both prototype cDMAs, operated at a sheath/aerosol flowrate ratio less than 15:1 and with a polydisperse aerosol flowrate of 1.0 lpm, achieved sizing resolution comparable to that offered by Nano-DMA. The longer cDMA had comparable transmission efficiency to that of Nano-DMA, and the shorter cDMA exceeded the performance of Nano-DMA. Hence, the cDMA with the shorter (1.75 cm) classification length is better suited for the characterization of macromolecular samples.

1. Introduction

Differential mobility analyzers (DMAs) are now considered the standard tools for studying particles in sub-micrometer and nanometer size ranges. The primary function of a DMA is to size or classify monodisperse particles based on their electrical mobility. The development of instruments based on electrical mobility techniques can be dated to the turn of the 20th century (McClelland, 1898; Ebert, 1901; Zeleny, 1900; McClelland and Kennedy, 1912). The early development stemmed from interest in measuring atmospheric ions. The history of DMA development using coaxially aligned cylindrical condensers to measure the mobility of air ions can be traced back to the early works of Zeleny (1898, 1900, 1929), Langevin (1902, 1903a, 1903b), and Langevin and Moulin (1907). The lengths of DMA columns were extended later

* Corresponding author. Tel.: +1 314 935 7924; fax: +1 314 935 5464.
E-mail address: chen@seas.wustl.edu (D.-R. Chen).

0021-8502/$ - see front matter © 2011 Elsevier Ltd. All rights reserved.
doi:10.1016/j.jaerosci.2011.04.001

for measuring particles with sizes larger than air ions. The early work and later development of DMAs were nicely reviewed in an article by Flagan (1998).

A DMA for measuring sub-micrometer particles was developed in the 1960s at the University of Minnesota (Knutson & Whitby, 1975a, 1975b; Whitby & Clark, 1966). In this instrument, electrically charged particles migrate across the annular spacing formed by two coaxial-aligned cylinders held at different constant electrical potentials, while clean sheath gas flowing in parallel to the axis forms a barrier to particle migration. The most used DMA is the one designed by Liu and Pui (1974), which was later commercialized by TSI Inc. (TSI model 3701).

Three basic configurations have been implemented in DMA design: cylindrical, radial, and parallel plate. Examples of cylindrical DMAs are the Hauke 3/150 (Winklmayr et al., 1991) and the Nano-DMA (Chen et al., 1998). The SMEC (Spectrometre de Mobilite Electrique Circulaire), developed by Pourpix and Daval (Pourpix and Daval, 1990; Pourprix, 1994), and the Radial DMA (RDMA) by Zhang et al. (1995) are examples of radial DMAs. Santos et al. (2009) developed a high-resolution parallel plate DMA especially for the measurement of ion mobility spectra. In general, the sizing performance of DMAs deteriorates as the size of the particles to be detected is reduced, especially for nanoparticles (Chen et al., 1996). Two different methods have been pursued in DMA design to improve the sizing performance. One design strategy is to shorten the classification length, such as in the Nano-DMA (Chen et al., 1998) and short RDMA (Brunelli et al., 2009). The other strategy to achieve high sizing resolution for particles in the sub-10 nm size range is to operate the DMA at high sheath flowrates, up to 2200 lpm, with Reynolds numbers up to 62,000 (de Juan & de la Mora, 1998; Eichler, 1997; Martinez-Lozano & de la Mora, 2006; Ramiro et al., 2003; Rosell-Llompart et al., 1996; Ramiro et al., 2004).

Other efforts have been made to widen the sizing range and to reduce the response time of DMAs. The adjustable column length DMA (ACLDMA) (Seol et al., 2002) was developed for variable sizing ranges. Multi-electrode DMAs (Mirme, 1994; Tammet et al., 2002) were also developed to reduce the DMA measurement time from minutes to a fraction of a second. Further, a multi-stage DMA (MDMA) was designed to extract monodisperse particles of different sizes at the same time (Chen et al., 2007). The MDMA not only covers a wide sizing range but also improves the DMA measuring cycle by varying the voltage in sub-sections of the entire sizing range.

The sizing ability of a DMA, in combination with particle concentration detectors (i.e., aerosol electrometers or condensation particle counters), allows us to measure the size distribution of particles in various areas of investigation, including air pollution and climate change, atmospheric aerosol transport, particulate material synthesis, particulate emission and control, indoor air quality (Salthammer & Uhde, 2009), and particle inhalation and toxicity (Grassian et al., 2007; Ji et al., 2007; Kulkami et al., 2008; Lee, 2006). Used as a classifier, a DMA can produce monodisperse particles for further investigation. Hirasawa et al. (2006) coupled a DMA with an electrospray aerosol generator (ES-DMA), and this instrument was used to characterize proteins, lipo-particles, and viruses based on their charge-to-aerodynamic size ratio (Allmaier et al., 2008; Benner et al., 2007; Pease et al., 2008). The ES-DMA is also known as a gas-phase electrophoretic mobility macromolecular analyzer, GEMMA (Bacher et al., 2001; Kaufman, 2000). Notice that the DMAs in the above-described applications are used primarily for particle characterization.

The low throughput of a DMA limits its use in industrial applications, for example, sorting biological macromolecules on an industrial scale. A simple way to scale up throughput is to use multiple DMA columns. In biological and pharmaceutical applications, the sizes of proteins, lipo-particles, and viruses are usually less than 20 nm. Although Nano-DMA (TSI 3085) is applicable to such macromolecular characterization, the cost of the column is relatively high, making it impractical for a multiple DMA column application. The objective of this work is thus to develop a cost-effective DMA with low maintenance that enables multiple DMA applications, especially for sorting biological macromolecules.

2. Design of prototype cDMA

The prototype cost-effective DMA (cDMA) is a cylindrical configuration with two aerosol inlets located at opposite positions on the DMA column, and one aerosol outlet for connection to an aerosol concentration detector, such as an aerosol electrometer (AE) or a condensation particle counter (CPC). As shown in Fig. 1, the structure of the cDMA consists of an outer cylinder with an inner diameter of 3/8″ (0.953 cm), and an inner rod with diameter of 3/16″ (0.476 cm). The inner rod is co-axially aligned with the outer cylinder. Polydisperse aerosol flow is introduced into the cDMA classification region via the two opposite inlets. Upon entering the inlets, the aerosol flow is quickly distributed in the annular chamber, formed by the conical cap and the dome surface below, and then transported to the annular slit for entering the particle classification region.

Clean sheath flow enters the cDMA from the top and passes through a metal honeycomb structure that distributes and laminates the sheath flow before it reaches the particle classification region. Polydisperse particles are introduced into the cDMA via the inlets and transported through a narrow annular slit before merging with the clean sheath flow in the classification region. The classified aerosol then exits via the flow channel in the inner rod. To minimize the pressure drop while ensuring uniform flow in the classification region, excess flow exits the cDMA via the chamber in the base.

As shown in Fig. 1, the classification length of the prototype cDMA can be easily varied by replacing just two metal pieces, A and B. Two classification lengths, 1.75 and 4.5 cm, were used in the performance evaluation of the prototype. The cDMA with 1.75 cm classification length (cDMA-1) was designed for particles smaller than 15 nm, and the one with 4.5 cm length (cDMA-2) for particles smaller than 50 nm.

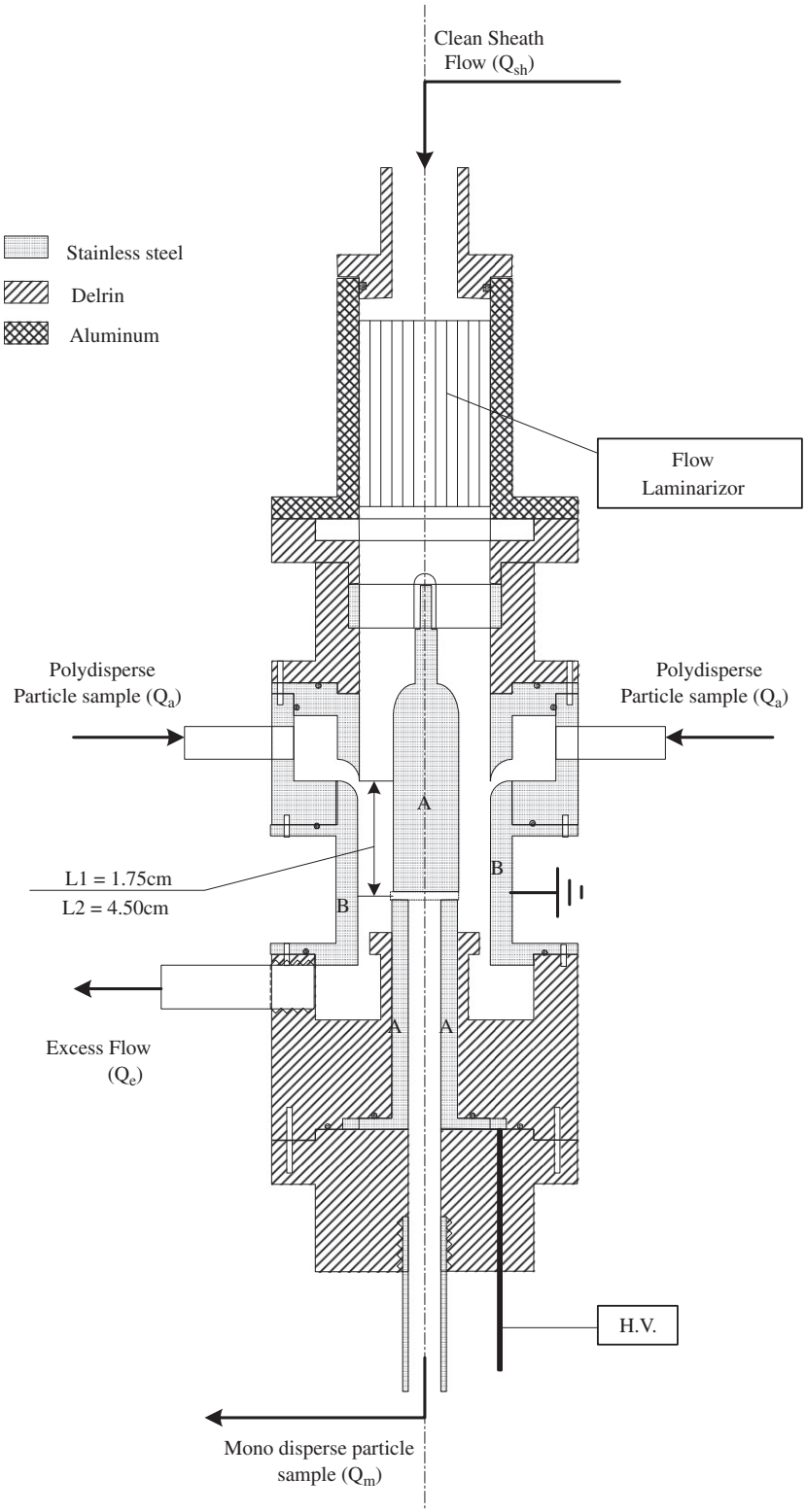

Fig. 1. Schematic diagram of economical DMAs (cDMAs).

The key components used for particle classification in cDMAs are smaller in diameter and shorter in classification length than in conventional DMAs. Hence, the cDMA design cost less to make. Further, a honing machine is required for DMA cylinders to provide the requisite straight and smooth inner surface for particle classification. The smaller diameter and shorter lengths of cDMA cylinders make honing easy, further reducing their manufacturing cost. The cDMA design also moves the donut-type laminar flow distributor (LFD) used in conventional DMAs out of the particle classification region. The LFD is often specially made for a particular DMA. The arrangement of cDMAs, however, makes often possible to fabricate an LFD cheaply. For instance, instead of using the LFDs in conventional DMAs, the LFD in the prototype cDMAs was in fact made from a bundle of 2 mm diameter coffee stirrers.

Therefore, several key features in the design of cDMAs facilitate part exchanges and reduce manufacturing cost, while providing performance comparable to that of conventional DMAs. The part count of cDMAs is less than existing DMAs, making the cDMAs easy to assamble and reducing maintenance effort and cost.

3. Experimental setup and procedure

3.1. Generation of monodisperse test particles

Fig. 2 is a schematic diagram of the particle generation system used in this study. A system employing evaporation, condensation, and DMA-classification was used to produce test monodisperse particles in desired sizes (Bartz et al., 1987; Scheibel & Porstendorfer, 1983).

To generate particles larger than 15 nm, sodium chloride powder (NaCl, ACS reagent, $\geq$ 99.0%, Sigma-Aldrich) was placed in a ceramic boat located in the ceramic tube of a high temperature tube furnace (Lindberg® Blue M® mini-Mite™ tube Furnace, Thermo Scientific) with a temperature setting of 600–700 °C. Filtered nitrogen gas at 0.5 lpm was passed through the ceramic tube to carry NaCl vapor out of the furnace. At the exit of the furnace tube, a cool stream of nitrogen at 0.2–1.0 lpm was mixed with the vapor-enriched stream. Polydisperse particles with a geometrical standard deviation (σ_g)

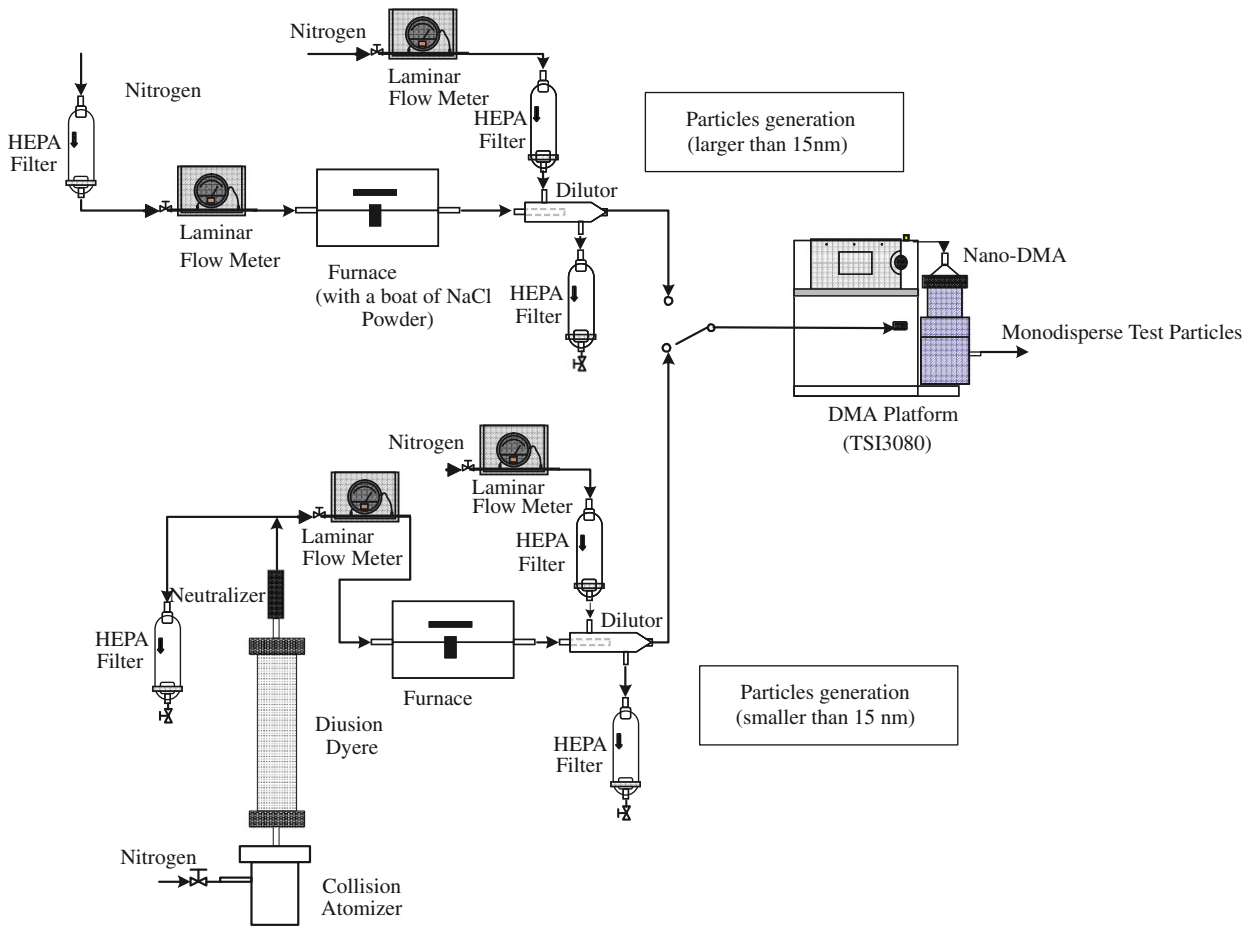

Fig. 2. Schematic diagram of the monodisperse particle generation system used in our study.

of approximately 1.45 then formed via homogeneous condensation. The mean sizes of the particles could be controlled by varying the furnace temperature and ratio of the two nitrogen flows. For particles smaller than 15 nm, a custom-made Collison atomizer, operating at a liquid volume consumption rate of 4 ml/h, was used to spray an aqueous NaCl solution. The water in the sprayed droplets was evaporated in a diffusion dryer with silicon desiccants before vaporization in the high temperature tube furnace. The furnace temperature was varied from 720 to 900 °C. A cool stream of nitrogen at flow rates ranging from 0.2 to 1.0 lpm was mixed with the hot stream downstream from the tube furnace. The mean sizes of particles generated depended on the initial NaCl concentration in the spray solutions, the furnace temperature, and the quenching flow rate. Polydisperse particles with a number mean diameter of about 11 nm were produced by spraying a 1% NaCl solution, setting the furnace temperature at 800 °C, and using a quenching flowrate of 0.5 lpm.

Polydisperse NaCl particles were then passed through a differential mobility classifier (Nano-DMA, TSI 3085) to obtain monodisperse test particles. The Nano-DMA was operated at a sheath-to-aerosol-flowrate ratio of 15:1. This high flowrate ratio yielded a narrower size distribution of monodisperse test particles for evaluation of the prototype cDMA. Seven particle sizes were selected for the evaluation: 5, 6, 8, 10, 15, 20, and 30 nm. For the cDMA-2, one more particle size, 50 nm, was also included in the evaluation.

3.2. Experimental setup

The transfer function of a DMA is best obtained by the Tandem DMA (TDMA) technique (Chen et al., 2007; Fissan et al., 1996; Hummes et al., 1996). In this study, we used the same technique to evaluate the performace of the cDMAs. Since two identical cDMAs were not available, we used a Nano-DMA (TSI 3085) as the first DMA in the TDMA system (shown in Fig. 2). Prior to evaluating the cDMAs, we checked the performance of the Nano-DMA using the TDMA technique.

In the TDMA experiment, the voltage applied to the first DMA was fixed for a desired particle size. The voltage on the second DMA was then scanned through the entire voltage range. An ultrafine condensation particle counter (TSI model 3025) was used to measure the particle concentration at the exit of the second DMA. The TDMA curve was derived by normalizing the concentration at the outlet of the second DMA (C_2) with the concentration at the exit of the first DMA (C_1). Based on our experimental results, the empirical parameters of the Nano-DMA transfer function in our test were in good agreement with the data given by Fissan et al. (1996).

To evaluate the performance of a cDMA, we replaced the second Nano-DMA in the TDMA setup with a cDMA. Fig. 3 shows the part of the TDMA setup related to a cDMA. The polydisperse and monodisperse aerosol flow rates of the cDMA were both monitored by laminar flowmeters. In this study we kept the aerosol flowrates at 1.0 lpm. Two mass flow meters (TSI Model 4000) were used to monitor the sheath and excess flow rates of the cDMA. A high-voltage power supply (Bertan Model 206B-10R) was used to apply the voltage on the cDMA. Again, we used an ultrafine condensation particle counter (UCPC, TSI 3025A) as the particle concentration detector. The UCPC was operated at the high flowrate (1.5 lpm).

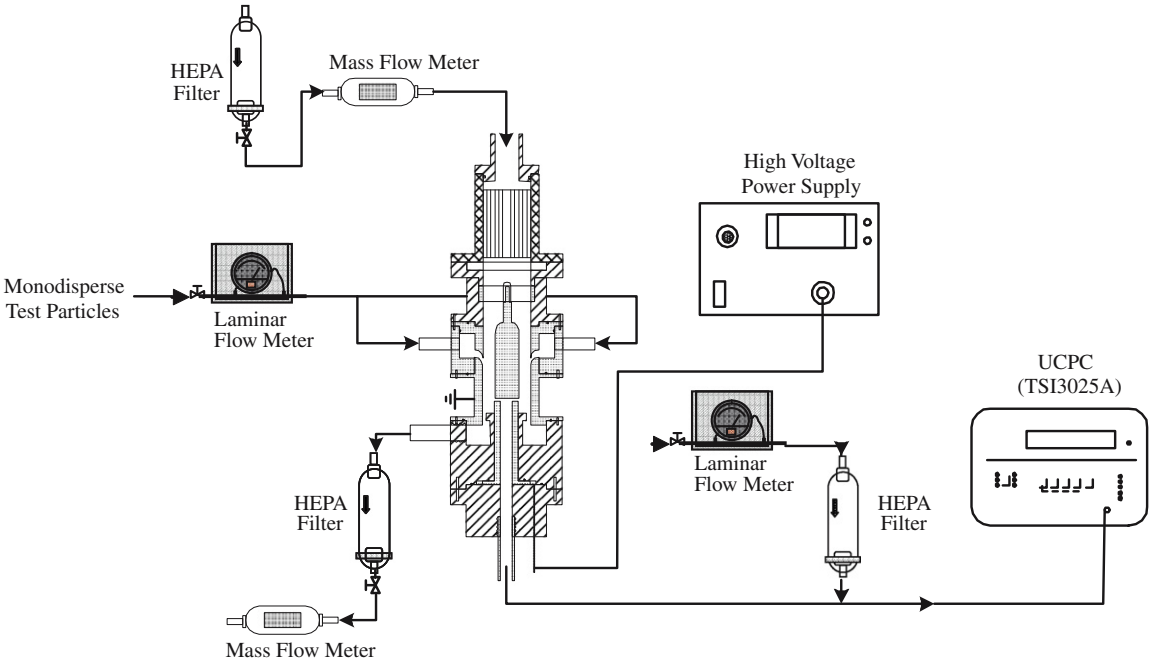

Fig. 3. Schematic diagram of the part of TDMA setup used for the performance evaluation of cDMAs.

A tee-connector was used before the UCPC sampling inlet to admit the additional particle-free flow needed for high flowrate operation of the UCPC. Particles in the additional flow were removed by a HEPA cartridge, and its flow rate was controlled by a laminar flow meter and needle valve.

3.3. Deconvolution scheme for cDMA transfer function

In principle, the experimental TDMA curve is the result of the convolution of the two DMA transfer functions. A deconvolution scheme is thus required to recover the DMA transfer function. In the traditional schemes, to minimize the effect of error propagation, it is recommended to use two identical DMA columns operated at identical aerosol and sheath flowrates. The conventional deconvolution scheme typically assumes the shape of the transfer function to be either triangular or Gaussian (Hummes et al., 1996; Stratmann et al., 1997). The full width at half maximum and the height are two parameters characterizing the transfer function of the presumed functional forms. Both parameters can be found by fitting the calculated TDMA curve to the experimental one with a preset error tolerance.

Since the TDMA experimental curves obtained in this experiment were the convoluted results of the Nano-DMA and cDMA transfer functions, a piecewise-linear function deconvolution scheme (Li et al., 2006) was used to recover the true transfer function of the cDMA, given the real transfer function of the Nano-DMA. In the scheme, the electrical mobility window of a DMA transfer function is divided into N evenly distributed subsections, and the variation of the transfer function in each subsection is assumed linear. The entire DMA transfer function is thus represented as a piecewise linear function with $(N+1)$ parameters. The convoluted TDMA curve can be calculated from this representative transfer function. A numerical optimization scheme was applied to vary the values of the parameters simultaneously, minimizing the difference between the measured and calculated TDMA curves. The same deconvolution scheme has been applied to obtain the real transfer function of the Nano-DMA (Li et al., 2006) and MDMA (Chen et al., 2007).

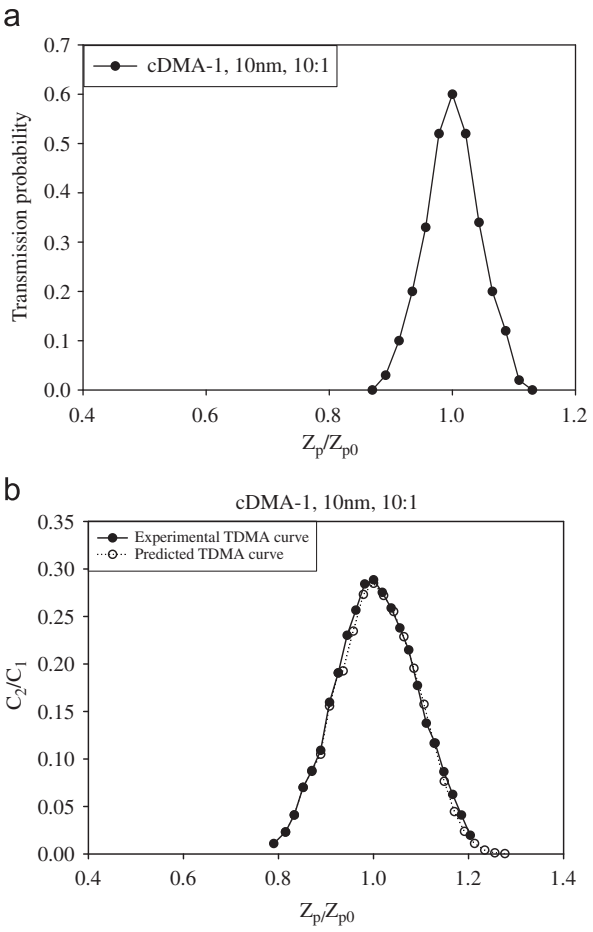

Fig. 4. (a) Typical transfer function of cDMA-1 for 10 nm particle size, obtained via the linear-piecewise function deconvolution scheme. (b) Comparison of experimental and calculated TDMA curves for cDMA-1. cDMA-1 was operated at the sheath/aerosol flowrate ratio of 10.

4. Results and discussion

4.1. Typical transfer function of cDMAs

Fig. 4(a) shows a typical transfer function for cDMA-1, operated at aerosol and sheath flow rates of 1 and 10 lpm, respectively. Using the scheme proposed by Li et al. (2006), the transfer function was obtained by best fitting the calculated TDMA curve with the measured one. The good agreement between the calculated and experimental TDMA curves is evident in Fig. 4(b). The shape of the transfer function is nearly triangular, and the maximum transmission probability of the function is 0.6. Fig. 5(a) gives a typical transfer function of cDMA-2 for 20 nm particles, operated at the same flow rates described above. As expected, the shape of the cDMA-2 transfer function for 20 nm particles was triangular, and the maximum transmission probability of the transfer function was 0.56. The good agreement between the calculated and measured TDMA curves for this case is shown in Fig. 5(b).

4.2. Sizing accuracy of cDMAs

Based on DMA theory (Knutson & Whitby, 1975a), the central mobility of test particles can be calculated by

$$Z_p^* = \left(\frac{Q_c + Q_m}{4\pi LV}\right)\ln(r_2/r_1), \tag{1}$$

where Q_c and Q_m are the sheath flow and excess flow rates, respectively; V is the voltage applied on the DMA central electrode; L is the effective classification length; and r_1 and r_2 are the inner radii of the rod and outer cylinder, respectively.

In the experiment, test particles classified by the Nano-DMA were introduced into a cDMA. The particle concentration at the cDMA monodisperse aerosol outlet was measured at various cDMA voltages. For a given geometry and operating

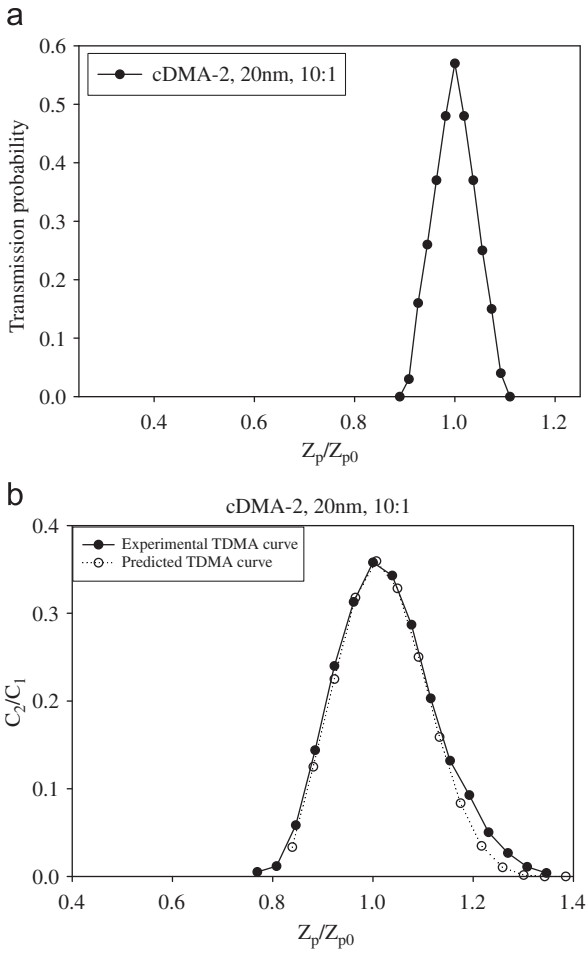

Fig. 5. (a) Typical transfer function of cDMA-2 for 20 nm particle size, obtained via the linear-piecewise function deconvolution scheme. (b) Comparison of experimental and calculated TDMA curves for the cDMA-2. cDMA-2 was operated at the sheath/aerosol flowrate ratio of 10.

conditions, the voltage of a cDMA can be calculated via Eq. (1) for a given particle electrical mobility. Fig. 6 shows the ratios of calculated voltage (V_c) to the measured voltage (V_m) at the peak particle concentration for both cDMAs. The fact that the ratios at various particle sizes are close to 1 for both cDMAs indicates that they operate as designed. Taking into consideration the flowrate measurement accuracy and machining tolerance of the cDMA, it is reasonable to estimate that the relative error of the particle electrical mobility measurement should be less than 3%.

4.3. Sizing resolution of cDMAs

The full width at half of the maximum height of a DMA transfer function for non-diffusive particles is predicted by Eq. (2).

$$\text{Half}-\text{width} = \beta \times (1+\delta), \tag{2}$$

where $\beta=(Q_s+Q_a)/(Q_c+Q_m)$, and $\delta=(Q_s-Q_a)/(Q_s+Q_a)$. Here, Q_a, Q_s, Qc and Qm are the flowrates of polydisperse aerosol, monodisperse aerosol, sheath gas, and excess flow, respectively. In this study, the sizing resolution of a cDMA for a given particle size is presented as the inverse of the half-width of the experimental DMA transfer function.

Fig. 7 shows the sizing resolution obtained from the transfer functions of both cDMAs as a function of particle size, when the cDMAs were operated at sheath flows of 5.0, 10.0, and 15.0 lpm. The polydisperse aerosol flow was 1.0 lpm, and the aerosol sampling flow was 1.0 lpm. Based on these operating conditions, the ideal resolutions for non-diffusive particles in the above cases are 5, 10, and 15 for the flowrate ratios of 5:1, 10:1 and 15:1, respectively. However, because of particle Brownian diffusion, for the three tested flowrate ratios, the cDMA resolution decreased with a decrease in the particle size. Compared with cDMA-2, the cDMA-1 (with the shorter particle classification length) resulted in reduced particle residence time, consequently leading to the highest sizing resolution for a given particle size. As evidenced in Fig. 7, the sizing resolutions at all three test flowrate ratios approach the ideal values as the particle size increases.

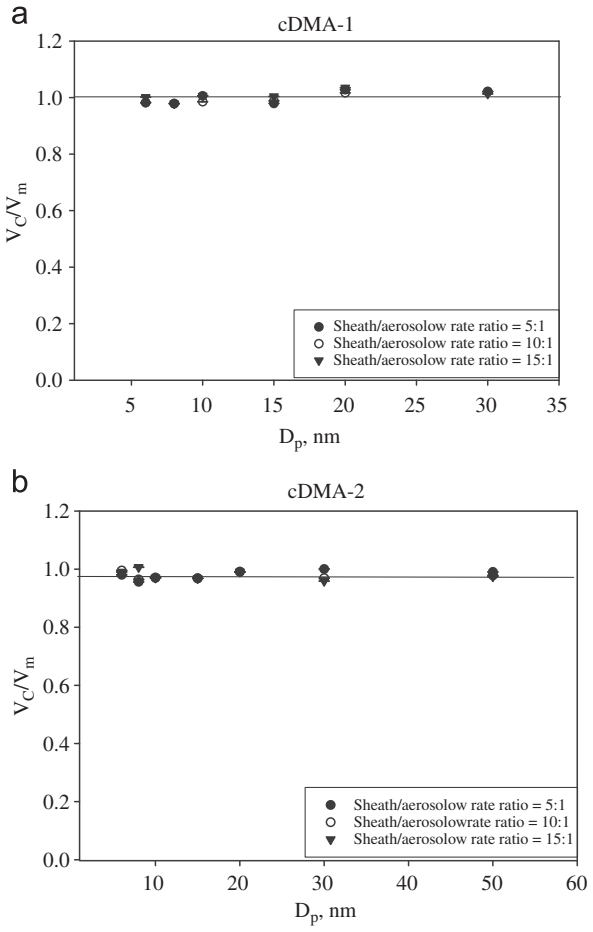

Fig. 6. Ratios of calculated and measured central voltages for cDMA operating at the ratio of sheath/aerosol flowrate as 5, 10, and 15: (a) for cDMA-1 and (b) for cDMA-2.

The good agreement between the experimental and theoretical values in sizing resolution evidences the proper design of the cDMAs.

Note that, as shown in Fig. 7, a discrepancy was observed between the ideal and experimental sizing resolution data at the flowrate ratio of 15:1. The discrepancy was possibly the result of (1) particle loss, (2) flow disturbance, and (3) experimental error and its propagation in the deconvolution scheme. Compared with the cases for flowrate ratios of 5 and 10, more particle loss was encountered when the flowrate ratio was 15. The higher particle loss lowered the maximum of the transfer function and consequently led to the decrease in the sizing resolution. Further, when a cDMA is operated with an increased velocity difference between the polydisperse aerosol and sheath flows, flow disturbance is more likely to occur near the flow matching region. In addition, experimental errors could result from the measurements of flowrate and particle concentration. The derived sizing resolution from the experimental data might be more sensitive to such errors when the electrical mobility window of the TDMA curves is relatively narrow.

4.4. Transmission efficiency of cDMAs

In addition to the sizing resolution, the other important parameter for DMA performance is the transmission efficiency, defined as the area ratio of the experimental transfer function to the ideal one. Transmission efficiency indicates particle loss in a DMA. In general, such particle loss is primarily due to the effects of particle diffusion and electrostatic loss. If we consider only the transfer function broadening due to particle diffusion, without the particle loss, then the area under the transfer function would remain the same while its height would be reduced. If we further take the particle loss into consideration, the area under the DMA transfer function would be less than that of the function for the case without particle loss.

For cases in which the polydisperse flowrate is equal to that of monodisperse aerosol flow, and the sheath flowrate is the same as that of excess flow, the ideal DMA transfer function for non-diffusive particles would be a triangle with

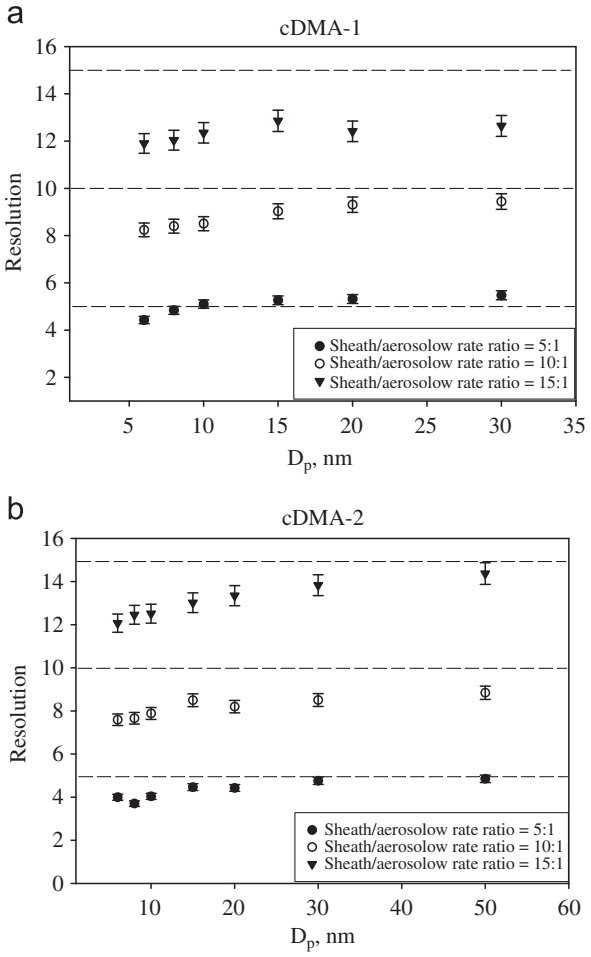

Fig. 7. Comparison of the sizing resolution (i.e., inversely half-width of the transfer function) of cDMAs at the sheath/aerosol flowrate ratios of 5, 10, and 15: (a) for cDMA-1 and (b) for cDMA-2.

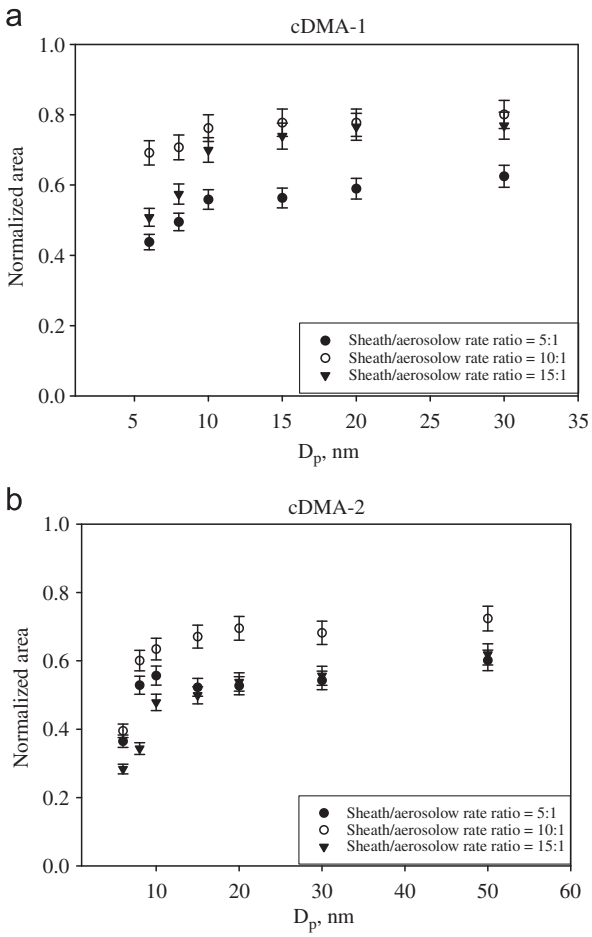

Fig. 8. Comparison of the normalized area of the cDMA transfer functions at the sheath/aerosol flowrate ratios of 5, 10, and 15: (a) for cDMA-1 and (b) for cDMA-2.

a height of 1.0 and half-widths of 0.2, 0.1, and 0.0667 for flowrate ratios of 5, 10, and 15, respectively. The corresponding function areas would be 0.2, 0.1, and 0.0667 (Knutson & Whitby, 1975b; Stolzenberg, 1998).

Fig. 8 shows the normalized area of the cDMA transfer function versus the particle size at three sheath/aerosol flowrate ratios for both cDMAs. The normalized area decreases with a decrease in particle size, because of the higher diffusion loss of the smaller particles. It is also observed that the normalized area increased when the sheath/aerosol flowrate ratio was increased from 5 to 10. However, the normalized area was reduced when the sheath/aerosol flowrate ratio was increased to 15. At this higher sheath/aerosol flowrate ratio, the flow inside the classification region is near the onset of laminar flow transient to turbulent flow. We believe that the disturbance of the laminar sheath flow contributes to both the uncertainty in the flow measurements and higher particle loss, suppressing the potential increase of transmission efficiency because of the increased sheath/aerosol flowrate ratio. Meanwhile, a high electrical field is needed in a DMA to size/classify particles of the same electrical mobility at high sheath flow operation. The strong electrical force may result in increased particle loss in both the aerosol inlet and outlet regions.

5. Conclusions

A new DMA column (cost-effective DMA or cDMA) has been successfully developed for multiple DMA column applications, and its performance has been calibrated by the tandem DMA (TDMA) technique. Two prototype cDMAs, with classification lengths of 1.75 and 4.50 cm (cDMA-1 and -2, respectively) were constructed. cDMA-1, with the shorter classification length, was designed for particles smaller than 30 nm. Users can easily customize their own length for a desired particle size range. Further, without sacrificing its performance, the cDMA design was manufactured economically from parts that required little machining.

A TDMA experimental setup was used to calibrate the performance of the cDMAs. For both cDMAs, the sizing resolution for large particle sizes was close to the theoretical values calculated by the non-diffusive model at flowrate ratios of 5 and 10. At a flowrate ratio of 15, cDMA-2 had better sizing resolution than cDMA-1, possibly because the flow disturbance caused

by the high flowrate ratio more adversely affected the performance of cDMA-1. For particles smaller than 20 nm, the sizing resolution of cDMA-2 was lower than that of cDMA-1 for all three flowrate ratios. Thus, cDMA-1 performs better for nanoparticle analysis than cDMA-2.

The particle transmission efficiency (i.e., normalized area) of both cDMAs in general follows the expected trend, decreasing as the particle size decreases. The transmission efficiency of cDMA-2 was comparable with that of Nano-DMA (Fissan et al., 1996; Chen et al., 1998) for the flowrate ratios of 5 and 10. In comparison, the efficiency of cDMA-2 was lower than that of the cDMA-1. The maximum transmission efficiency of cDMA-1 remained at 0.81. Hence, the cDMA with a shorter classification length (1.75 cm) is better suited for characterizing macromolecular samples.

Acknowledgment

The authors are grateful for the partial financial support provided by GeneSeek Inc. for this DMA development.

References

Allmaier, G., Laschober, C., & Szymanski, W.W. (2008). Nano ES GEMMA and PDMA, new tools for the analysis of nanobioparticles–protein complexes, lipoparticles, and viruses. *Journal of the American Society for Mass Spectrometry*, *19*, 1062–1068.

Bacher, G., Szymanski, W.W., Kaufman, S.L., Zollner, P., Blaas, D., & Allmaier, G. (2001). Charge-reduced nano electrospray ionization combined with differential mobility analysis of peptides, proteins, glycoproteins, noncovalent protein complexes and viruses. *Journal of Mass Spectrom*, *36*, 1038–1052.

Bartz, H., Fissan, H., & Liu, B.Y.H. (1987). A new generator for ultrafine aerosols below 10 nm. *Aerosol Science and Technology*, *6*, 163–171.

Benner, W.H., Krauss, R.M., & Blanche, P.J. (2007). *Ion Mobility Analysis of Lipoproteins*. United States Patent 7,259,018.

Brunelli, N.A., Flagan, R.C., & Giapis, K.P. (2009). Radial differential mobility analyzer for one nanometer particle classification. *Aerosol Science and Technology*, *43*, 53–59.

Chen, D.R., Li, W.L., & Cheng, M.D. (2007). Development of a multiple-stage differential mobility ananlyzer (MDMA). *Aerosol Science and Technology*, *41*, 217–230.

Chen, D.R., Pui, D.Y.H., Hummes, D., Fissan, H., Quant, F.R., & Sem, G.J. (1996). Nanometer differential mobility analyzer (Nano-DMA): Design and numerical modeling. *Journal of Aerosol Science*, *27*, S137–S138.

Chen, D.R., Pui, D.Y.H., Hummes, D., Fissan, H., Quant, F.R., & Sem, G.J. (1998). Design and evaluation of a nanometer aerosol differential mobility analyzer (Nano-DMA). *Journal of Aerosol Science*, *29*, 497–509.

de Juan, L., & de la Mora, J.F. (1998). High resolution size analysis of nanoparticles and ions: Running a Vienna DMA of near optimal length at Reynolds numbers up to 5000. *Journal of Aerosol Science*, *29*, 617–626.

Ebert, H. (1901). Aspriationsapparat zur bcstimmung des ionengehaltes dcr atmosphäre. *Zeitschrift für Physik*, *2*, 662–664.

Eichler, T. (1997). *A Differential Mobility Analyzer for Ions and Nanoparticles: Laminar Flow at High Reynolds Numbers*. Senior Graduate Thesis, Fachhochscule Offenburg, Germany.

Flagan, R.C. (1998). History of electrical aerosol measurements. *Aerosol Science and Technology*, *28*, 301–380.

Fissan, H., Hummes, D., Stratmann, F., Buscher, P., Neumann, S., Pui, D.Y.H., & Chen, D. (1996). Experimental comparison of four differential mobility analyzers for nanometer aerosol measurements. *Aerosol Science and Technology*, *24*, 1–13.

Grassian, V.H., O'Shaughnessy, P.T., Adamcakova-Dodd, A., Pettibone, J.M., & Thorne, P.S. (2007). Inhalation exposure study of titanium dioxide nanoparticles with a primary particle size of 2 to 5 nm. *Environmental Health Perspectives*, *115*, 397–402.

Hirasawa, M., Orii, T., & Seto, T. (2006). Size-dependent crystallization of Si nanoparticles. *Applied Physics Letters*, *88*, 093119.

Hummes, D., Stratmann, F., Neumann, S., & Fissan, H. (1996). Experimental determination of the transfer function of a differential mobility analyzer (DMA) in the nanometer size range. *Particle & Particle Systems Characterization*, *13*, 327–332.

Ji, J.H., Jung, J.H., Kim, S.S., Yoon, J.U., Park, J.D., Choi, B.S., Chung, Y.H., Kwon, I.H., Jeong, J., Han, B.S., Shin, J.H., Sung, J.H., Song, K.S., & Yu, I.J. (2007). Twenty-eight-day inhalation toxicity study of silver nanoparticles in Sprague the Dawley rats. *Inhalation Toxicology*, *19*, 857–871.

Kaufman, S.L. (2000). Electrospray diagnostics performed by using sucrose and proteins in the gas-phase electrophoretic mobility molecular analyzer (GEMMA). *Analytica Chimica Acta*, *406*, 3–10.

Knutson, E.O., & Whitby, K.T. (1975a). Aerosol classification by electric mobility: Apparatus, theory, and applications. *Journal of Aerosol Science*, *6*, 443–451.

Knutson, E.O., & Whitby, K.T. (1975b). Accurate measurerncnt of aerosol electric mobility moments. *Journal of Aerosol Science*, *6*, 453–466.

Kulkami, P., Deye, G.J., & Baron, P.A. (2008). Bipolar diffusion charging characteristics of single-wall carbon nanotube aerosol particles. *Journal of Aerosol Science*, *40*, 164–179.

Langevin, P. (1902). Sur la mobilitè des ions dans les gaz. *Conzptes Rendus*, *134*, 646–649.

Langevin, P. (1903a). L'Ionization des gaz. *Annals de Chimiset de' Physique*, *28*, 289–384.

Langevin, P. (1903b). Recombination et mobilitès des ions dans les gaz. *Annals de Chimie et de' Physique*, *28*, 433–530.

Langevin, P., & Moulin, M. (1907). Electromètre enregistreur des ions de l'atmosphère. *Le Radium*, *4*, 2l8–229.

Lee, Y. S. (2006). *Investigation of the Optical and Cloud Forming Properties of Pollution, Biomass Burning, and Mineral Dust Aerosols*. Dissertation in Texas A&M University.

Li, W., Li, L., & Chen, D.R. (2006). A new deconvolution scheme to recover the true DMA transfer function from TDMA curves. *Aerosol Science and Technology*, *40*, 1052–1057.

Liu, B.Y.H., & Pui, D.Y.H. (1974). A submicron aerosol standard and the primary, absolute calibration of the condensation nucleus counter. *Journal of Colloid Interface Science*, *47*, 155–171.

Martinez-Lozano, P., & de la Mora, J.F. (2006). Resolution improvements of a nano-DMA operating transonically. *Journal of Aerosol Science*, *37*, 500–512.

McClelland, J.A. (1898). On the conductivity of the hot gases from flames. *Philosophical Magazine*, *46*, 29–42.

McClelland, J.A, & Kennedy, H. (1912). *The Large Ions in the Atmosphere*, *Proceedings* of *the Royal Irish Academy* (*Vol. 30*, pp. 72–91).

Mirme, A. (1994). *Electric Aerosol Spectrometry*. PhD Thesis, University of Tartu.

Pease, L.F., Elliott, J.T., Tsai, D.H., Zachariah, M.R., & Tarlov, M.J. (2008). Determination of protein aggregation with differential mobility analysis: Application to IgG antibody. *Biotechnology and Bioengineering*, *101*, 1214–1222.

Pourprix, M. (1994). *Sélecteur de particules chargées, a haute sensibilité*, Brevet francais No. 94 06273, 24 Mal.

Pourpix, M., & Daval, J. (1990). Electrostatic precipitation of aerosol on wafers, a new mobility spectrometer. In: S. Masuda, & K. Takahashi (Eds.), *Aerosols: Science, Industry, Health and Environment. Proceedings of the Third International Aerosol Conference* (*Vol. II*), 24–27 September, 1990, Kyoto, Japan, Oxford, UK: Pergamon Press.

Ramiro, E., Ramiro, F., Sanchez, M., Lazcano, J.A., de Juan, J., & de la Mora, J.F. (2003). A DMA of inverted geometry for high Reynolds number operation. *Journal of Aerosol Science*, *34*(S2), S915–S916.

Ramiro, E., Sánchez, M., Ramiro, F., de la Mora, J.F., & Martínez-Lozano, P. (2004). Experimental validation of a high resolution nano-DMA. *Journal of Aerosol Science*, *35*(S2), S749–S750.
Rosell-Llompart, J., Loscertales, I.G., Bingham, D., & delaMora, J.F. (1996). Sizing nanoparticles and ions with a short differential mobility analyzer. *Journal of Aerosol Science*, *27*, 695–719.
Salthammer, T., & Uhde, E. (Eds.). (2009). *Organic Indoor Air Pollutants: Occurrence, Measurement, Evaluation* (2nd ed.). WILEY-VCH: Weinheim.
Santos, J.P., Hontanon, E., Ramiro, E., & Alonso, M. (2009). Performance evaluation of a high-resolution parallel-plate differential mobility analyzer. *Atmospheric Chemistry and Physics*, *9*, 2419–2429.
Scheibel, H.G., & Porstendorfer, J. (1983). Generation of monodisperse Ag and NaCl aerosols with particle diameters between 2 and 300 nm. *Journal of Aerosol Science*, *14*, 113–126.
Seol, K.S., Yabumoto, J., & Takeuchi, K. (2002). A differential mobility analyzer with adjustable column length for wide particle-size-range measurements. *Journal of Aerosol Science*, *33*, 1481–1492.
Stolzenburg, M. (1998). PhD Thesis, Department of Mechanical Engineering, University of Minnesota, Minneapolis, MN.
Stratmann, F., Kauffeldt, Th., Hummes, D., & Fissan, H. (1997). Differential electrical mobility analysis: A theoretical study. *Aerosol Science and Technology*, *26*, 368–383.
Tammet, H., Mirme, A., & Tamm, E. (2002). Electrical aerosol spectrometer of Tartu university. *Atmospheric Research*, *62*, 315–324.
Whitby, K.T., & Clark, W.E. (1966). Electrical aerosol particle counting and size distribution measuring system for the 0.015 to 1 μ size range. *Tellus*, *18*, 573–586.
Winklmayr, W., Reischl, G.P., Linder, A.O., & Berner, A. (1991). A new electromobility spectrometer for the measurement of aerosol size distributions in the size range from 1 to 1000 nm. *Journal of Aerosol Science*, *22*, 289–296.
Zeleny, J. (1898). On the ratio of the velocities of the two ions produced in gases by rontgen radiation; and on some related phenomena. *Philosophical Magazine*, *46*, 120–154.
Zeleny, J. (1900). The velocity of the ions produced in gases by Rontgen rays. *Philosophical Transactions A*, *195*, 193–234.
Zeleny, J. (1929). The distribution of mobilities of ions in air. *Physical Review*, *34*, 310–334.
Zhang, S.H., Akutsu, Y., Russell, L.M., Flagan, R.C., & Seinfeld, J.H. (1995). Radial differential mobility analyzer. *Aerosol Science and Technology*, *23*, 357–372.